Physica A 561 (2021) 125297

Contents lists available at ScienceDirect

Physica A

journal homepage: www.elsevier.com/locate/physa

Shear zone instability of a 2d periodic Euler flow

Renato Pakter, Yan Levin *

Instituto de Física, UFRGS, Caixa Postal 15051, CEP 91501-970, Porto Alegre, RS, Brazil

ARTICLE INFO

Article history:
Received 13 June 2020
Available online 19 September 2020

ABSTRACT

It has been known for over 150 years that a shear flow can become unstable due to microscopic perturbations. The instability manifests itself in waves on water surface, in clouds, in sun's corona, and in the famous Jupiter's Red Spot. The traditional approach to study the linear stability of a flow is through the analysis of Euler's equations of fluid motion. In this paper we present an alternative approach which relies on the mapping of Euler's equations on an infinite system of interacting vortices. Using this approach we are able to predict the limits of stability of a shear layer of finite width confined to a cylindrical surface. We also predict the wavelength of the most unstable mode and compare it with the results of molecular dynamics simulations.

Kelvin–Helmholtz (KH) instability [1,2] is often the initial step that leads to a large scale vortex formation in 2d fluids undergoing a shear flow [3]. This process is believed to be responsible for the observed Jupiter's Great Red Spot, the origin of which is supposed to be the KH instability of the Jovian jets.

The KH linear instability is usually studied using a perturbative solution of 2d Euler equations [4,5]. Here we will present an alternative vortex formulation of the problem. The formalism is particularly useful for the exploration of the asymptotic structure of periodic flows using methods of non-equilibrium statistical mechanics of systems with long-range interactions [6,7]. This will be the subject of the future work.

In the planetary context the jets behave as a 2d Euler fluid confined to the surface of a sphere. To simplify the calculations, we will replace the spherical planetary geometry by an infinitely long cylinder of radius R. This is a reasonable approximation since the width of the equatorial jet streams is much smaller than the Jupiter's radius R. The cylindrical geometry is sufficiently simple that it will allow us to derive simple analytical expression for KH instability in a periodic flow. We note, however, that there are numerical studies of instabilities of vortex patches on a sphere, see for example Ref. [8].

The position on the surface of the cylinder can be written in terms of the angular and longitudinal variables, θ and z, as $\mathbf{r} = R\cos\theta\hat{\mathbf{x}} + R\sin\theta\hat{\mathbf{y}} + z\hat{\mathbf{z}}$. Consider a shear zone of width $2w$ such that the fluid velocity for $z > w$ is $-u_0$ and for $z < -w$ is u_0, with the velocity field varying linearly within the shear zone,

$$\mathbf{u}_0(\mathbf{r}) = -\hat{\boldsymbol{\theta}}\left[\frac{zu_0}{w}\,\Theta(w^2 - z^2) + u_0\,\mathrm{sign}(z)\Theta(z^2 - w^2)\right], \tag{1}$$

where $\Theta(x)$ is the Heaviside step function, see Fig. 1. The solution to the incompressible 2d Euler equation can be written in terms of a pseudo scalar vorticity $\Gamma(\mathbf{r}, t) = [\nabla \times \mathbf{u}(\mathbf{r}, t)] \cdot \hat{\boldsymbol{\rho}}$, where $\mathbf{u}(\mathbf{r}, t)$ is the velocity of fluid at position $\mathbf{r}$, and $\hat{\boldsymbol{\rho}}$ is the unit vector normal to the surface of the cylinder. It can be shown that the vorticity field is advected by the flow, $d\Gamma(\mathbf{r}, t)/dt = 0$. The incompressibility condition for the Euler equation allows one to introduce a stream function $\psi(\mathbf{r}, t)$ such that $\mathbf{u}(\mathbf{r}, t) = \nabla \times \psi(\mathbf{r}, t)\hat{\boldsymbol{\rho}}$ which satisfies the Poisson equation

$$\nabla^2\psi(\mathbf{r}, t) = -\Gamma(\mathbf{r}, t), \tag{2}$$

* Corresponding author.
E-mail address: levin@if.ufrgs.br (Y. Levin).

https://doi.org/10.1016/j.physa.2020.125297
0378-4371/

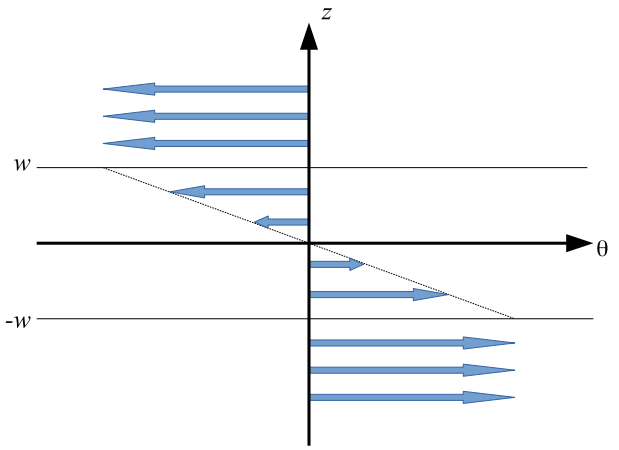

Fig. 1. Representation of shear flow given by Eq. (1).

the solution to which can be written in terms of an appropriate Green function,

$$\psi(\mathbf{r},t)=\int G(\mathbf{r},\mathbf{r}')\Gamma(\mathbf{r}',t)d\mathbf{r}'. \tag{3}$$

If we suppose that vorticity is composed of point vortices, $\Gamma(\mathbf{r})=\sum_i \Gamma_i\delta(\mathbf{r}-\mathbf{r}_i(t))$, their velocity must be the same as that of the fluid, $\dot{\mathbf{r}}_\mathbf{i}=\nabla_i\times\sum_{j\neq i}\Gamma_j G(\mathbf{r}_i,\mathbf{r}_j)\hat{\boldsymbol{\rho}}$ and we see that the vortex dynamics has a Hamilton-like structure [9]

$$\Gamma_i\dot{\theta}_i=\frac{1}{R}\frac{\partial\mathcal{H}}{\partial z_i}\;\;;\;\;\Gamma_i\dot{z}_i=-\frac{1}{R}\frac{\partial\mathcal{H}}{\partial\theta_i}\,, \tag{4}$$

where the Kirchhoff function [10] is defined as $\mathcal{H}=\sum_{i<j}\Gamma_i\Gamma_j G(\mathbf{r}_i,\mathbf{r}_j)$. The θ and z coordinates of a vortex are, therefore, conjugate variables.

The velocity field Eq. (1) is produced by the stream function

$$\psi_0(\mathbf{r})=-\frac{(w^2+z^2)u_0\Theta(w^2-z^2)+2w|z|u_0\Theta(z^2-w^2)}{2w}\,, \tag{5}$$

the source for which can be shown to be a water bag vorticity distribution,

$$\Gamma_0(\mathbf{r})=\gamma_0\Theta[w^2-z^2], \tag{6}$$

where $\gamma_0=u_0/w$, see Eq. (2). The total vortex strength of the shear flow is $\int\Gamma_0(\mathbf{r})d^2\mathbf{r}=4\pi Ru_0$. The strength of a point vortex is then $\Gamma_v=4\pi Ru_0/N$. The limit in which the vortex description of the fluid dynamics becomes exact is $\Gamma_v\to 0$, $N\to\infty$, with $N\Gamma_v$ held fixed at $4\pi Ru_0$.

The periodic Green function for Poisson equation (2) can be easily calculated [11,12] and is found to be

$$G(\mathbf{r},\mathbf{r}')=-\frac{|z-z'|}{4\pi R}+\sum_{n=1}^{\infty}\frac{e^{\frac{-n|z-z'|}{R}}}{2\pi n}\cos[n(\theta-\theta')]\,, \tag{7}$$

which can be explicitly summed to

$$G(\mathbf{r},\mathbf{r}')=-\frac{1}{4\pi}\log\left[2\cosh\left(\frac{|z-z'|}{R}\right)-2\cos(\theta-\theta')\right]. \tag{8}$$

To verify the conditions for the KH instability of a shear zone of width $2w$, we consider that the boundaries of the initial water bag vorticity distribution are perturbed

$$\Gamma(\mathbf{r},t)=\gamma_0\Theta\left[z^u(\theta,t)-z\right]\Theta\left[z^l(\theta,t)+z\right], \tag{9}$$

where $z^u(\theta,t)=w+\mathcal{F}^u(\theta,t)$ and $z^l(\theta,t)=w+\mathcal{F}^l(\theta,t)$ are the upper and the lower boundaries of the perturbed distribution and

$$\mathcal{F}^j(\theta,t)=\sum_{n=1}^{\infty}a_n^j(t)\cos(n\theta)+b_n^j(t)\sin(n\theta), \tag{10}$$

with $j=\{u,l\}$, and $a_n^j(t)$ and $b_n^j(t)$ being small amplitudes. Note that the form of the perturbation in Eq. (10) guarantees that the total volume occupied by the vorticity distribution is conserved, in agreement with the incompressibility of the

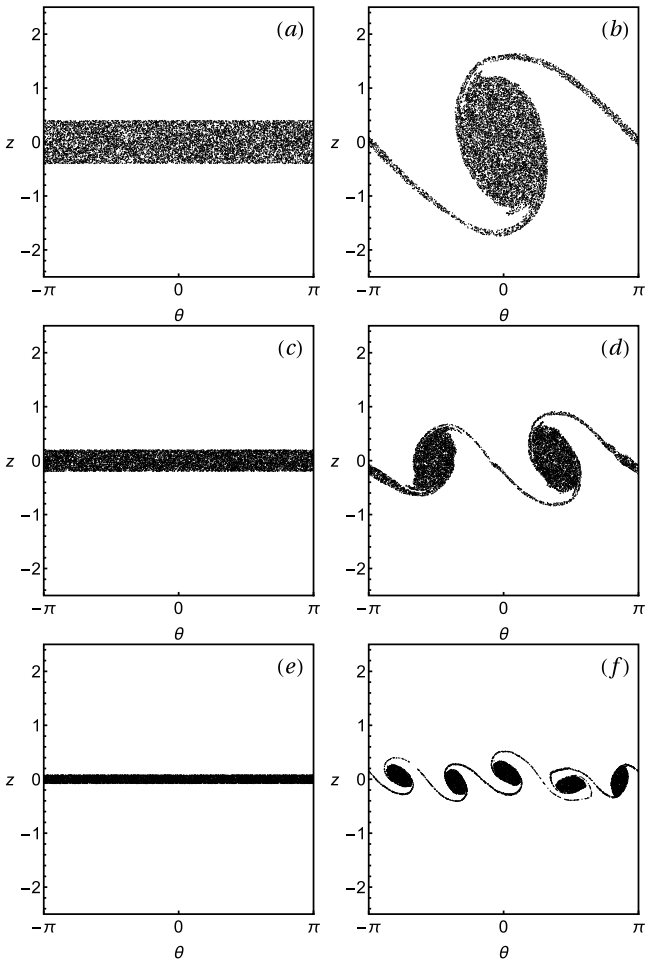

Fig. 2. Snapshots of molecular dynamics simulations with $N = 10^5$ vortices. The initial, panels (a), (c), and (e); and intermediate — after linear instability has taken place, panels (b), (d) and (f) — stages of the vortex evolution. After the linear instability takes place, the point vortices organize into macroscopic vortex structures, panels (b), (d) and (f). The initial water bag distribution in panel (a) has $w/R = 0.4$, for which the theory predicts the most unstable mode to be $n = 1$, resulting in one macroscopic vortex, panel (b). For panel (c), $w/R = 0.2$ and the most unstable mode is $n = 2$, resulting in the formation of two macroscopic vortices, panel (d). For panel (e) $w/R = 0.08$ and the most unstable mode is $n = 5$, resulting in the formation of five macroscopic vortices, panel (f). The longitudinal coordinate z is measured in units of R.

vortex dynamics. Expanding the vorticity distribution function of Eq. (9) up to linear terms in the perturbation amplitudes we obtain $\Gamma(\mathbf{r}, t) = \Gamma_0(\mathbf{r}) + \Gamma_1(\mathbf{r}, t)$, where

$$\begin{aligned}\Gamma_1(\mathbf{r}, t) = \gamma_0[&\delta(w - z)\Theta(w + z)\mathcal{F}^u(\theta, t) + \\ &\Theta(w - z)\delta(w + z)\mathcal{F}^l(\theta, t)],\end{aligned} \tag{11}$$

and $\delta(x)$ is the Dirac delta function. Substituting the perturbed distribution in Eq. (3) we find $\psi(\mathbf{r}, t) = \psi_0(\mathbf{r}) + \psi_1(\mathbf{r}, t)$ for the stream function, where

$$\begin{aligned}\psi_1(\mathbf{r}, t) = \sum_{n=1}^{\infty}\Bigg\{&\frac{e^{-\frac{n|w+z|}{R}}[a_n^l(t)\cos(n\theta) + b_n^l(t)\sin(n\theta)]}{8\pi n w} + \\ &\frac{e^{-\frac{n|w-z|}{R}}[a_n^u(t)\cos(n\theta) + b_n^u(t)\sin(n\theta)]}{8\pi n w}\Bigg\}.\end{aligned} \tag{12}$$

If we now impose that the vertical motion of the boundaries is consistent with the generated stream function (up to linear order in the amplitudes), i.e., $dz^j/dt = -(1/R)\partial\psi/\partial\theta|_{z=z^j}$, we obtain a closed set of linear equations for the perturbation

amplitudes. These equations can be written as $d\mathbf{C}_n/dt = \mathcal{M}_n \cdot \mathbf{C}_n$, where $\mathbf{C}_n = (a_n^l\ b_n^l\ a_n^u\ b_n^u)^T$ and

$$\mathcal{M}_n = \frac{\eta_0}{2}\begin{pmatrix} 0 & \alpha_n & 0 & \beta_n \\ -\alpha_n & 0 & -\beta_n & 0 \\ 0 & -\beta_n & 0 & -\alpha_n \\ \beta_n & 0 & \alpha_n & 0 \end{pmatrix}, \tag{13}$$

with $\alpha_n = 1 - 2nw/R$, $\beta_n = e^{-2nw/R}$. To write these expressions use has been made of $d\theta/dt|_{z^j} = \pm u_0/R$, to zeroth order in the perturbing amplitudes for the lower and the upper boundaries, respectively. The eigenvalues of $\mathcal{M}_n$ are given by $\gamma_n = \pm\eta_0\sqrt{\beta_n^2 - \alpha_n^2}/2$, and correspond to the exponential growth rate of the perturbations. Therefore, whenever $\beta_n^2 > \alpha_n^2$, a mode n is unstable, growing exponentially as the time evolves. In particular, for *large* w/R, all modes are stable. However when this ratio decreases below $w/R \approx 0.64$, the first mode $n = 1$ becomes unstable. Decreasing w/R even further destabilizes an increasing number of modes. The mode with the largest growth rate γ_n is expected to dominate the instability. More specifically, maximizing γ_n with respect to nw/R, we see that the fastest growing mode satisfies $n \approx 0.40/(w/R)$.

To explore the accuracy of the theory we have performed extensive molecular dynamics simulations using Vortex-in-Cell (VIC) algorithm [13–16]. In this approach the dynamics of $N = 10^5$ point vortices is solved using a Runge–Kutta (RK) algorithm with an adaptive time step, and the Poisson equation (2) is solved on a 500×500 mesh using a Successive Over-Relaxation (SOR) method [17]. We have checked that the results do not change with a further increase in the grid resolution and with the number of particles, showing that we have achieved the thermodynamic limit. We note that there are alternative methods which use contour dynamics to study instability of vortex patches and sheets [18–20], however our VIC simulations already provide us with enough resolution to explore the instability of a periodic shear flow. In Fig. 2 we show the snapshots of the evolution of a vortex distribution starting from an initial water bag distribution with different values of w/R. As predicted by the theory, the water bag distributions with $w/R > 0.64$ remain stable. For $w/R = 0.4$, the initial distribution in Fig. 2a becomes unstable. For this value of w/R, the theory predicts the most unstable mode to be $n = 1$. This is precisely what we find in simulations, see panel (b), which shows formation of one macroscopic vortex. In Fig. 2c the initial water bag distribution has $w/R = 0.2$ for which the most unstable mode is found to be $n = 2$, which again agrees perfectly with the simulations, see panel (d). Finally in Fig. 2e, we show the temporal evolution of the initial water bag distribution with $w/R = 0.08$. For such initial condition the most unstable mode is predicted to be $n \approx 0.40/0.08 = 5$, which agrees with the simulation showing formation of 5 macroscopic vortex blobs, see Fig. 2f.

We have presented an approach which allows us to obtain both the threshold of instability and to predict the wavelength of the most unstable mode of a 2d Euler fluid subjected to a shear flow in a cylindrical geometry. We find that the instability results in formation of n large scale vortices which after some time agglomerate into one macroscopic vortex. In the future work we will use the recently developed methods of non-equilibrium statistical mechanics [6] to attempt to predict the fluid velocity profile in the final stationary state, without explicitly solving Euler's equations of motion.

Declaration of competing interest

The authors declare that they have no known competing financial interests or personal relationships that could have appeared to influence the work reported in this paper.

Acknowledgments

This work was partially supported by the CNPq, National Institute of Science and Technology Complex Fluids INCT-FCx, and by the US-AFOSR, USA under the grant FA9550-16-1-0280.

References

[1] Lord Kelvin, W. Thomson, Phil. Mag. 42 (1871) 362.
[2] Hermann von Helmholtz, Mon.ber. K. Preuss. Akad. Wiss. Berl. 23 (1868) 215.
[3] P. Saffman, Vortex Dynamics, in: Cambridge Monographs on Mechanics, Cambridge University Press, 1993.
[4] J. Rayleigh, Proc. Lond. Math. Soc. 12 (1880) 57.
[5] P.K. Kundu, I.M. Cohen, Fluid Mechanics, fourth ed., Academic Press, New York, 2008.
[6] Y. Levin, R. Pakter, F.B. Rizzato, T.N. Teles, F.P.C. Benetti, Phys. Rep. 535 (2014) 1.
[7] R. Pakter, Y. Levin, Phys. Rev. Lett. 121 (2018) 020602.
[8] L.M. Polvani, D.G. Dritschel, J. Fluid Mech. 255 (1993) 35.
[9] P.K. Newton, The N-Vortex Problem, in: Applied Mathematical Sciences, vol. 145, Springer, New York, NY, 2001.
[10] G. Kirchhoff, Vorlesungen Über Mathematische Physik, Vol. 1, Teubner, Leipzig, 1883.
[11] H. Lamb, Hydrodynamics, sixth ed., Cambridge University Press, 1932.
[12] A.P. dos Santos, M. Girotto, Y. Levin, J. Chem. Phys. 147 (2017) 184105.
[13] J.P. Christiansen, J. Comput. Phys. 13 (1973) 363.
[14] J.P. Christiansen, N.J. Zabusky, J. Fluid Mech. 61 (1973) 219.
[15] D.G. Dritschel, R.K. Scott, C. Macaskill, G.A. Gottwald, C.V. Tran, Phys. Rev. Lett. 101 (2008) 094501.

[16] D.G. Dritschel, R.K. Scott, C. Macaskill, G.A. Gottwald, C.V. Tran, J. Fluid Mech. 640 (2009) 215.
[17] W.H. Press, B.P. Flannery, S.A. Teukolsky, W.T. Vetterling, Numerical Recipes in C: The Art of Scientific Computing, Cambridge Univ. Press, Cambridge, 1988.
[18] N.J. Zabusky, M.H. Hughes, K.V. Roberts, J. Comput. Phys. 30 (1979) 96.
[19] C. Pozrikidis, J.J.L. Higdon, J. Fluid Mech. 157 (1985) 225.
[20] G.R. Baker, M.J. Shelley, J. Fluid Mech. 215 (1990) 161.